NANOSYSTEMS:
PHYSICS, CHEMISTRY, MATHEMATICS

Rai R.K., Botet R.S. *Nanosystems: Phys. Chem. Math.*, 2022, **13** (1), 56–61.
http://nanojournal.ifmo.ru
**DOI 10.17586/2220-8054-2022-13-1-56-61**

Original article

# Near-field optical patterns of dielectric nanoparticles deposited on a metallic surface

Rakesh K. Rai[1,a], Robert S. Botet[2,b]

[1]B. R. A. Bihar University, Muzaffarpur, India
[2]Université Paris-Saclay, Orsay, France

[a]rakesh2273@gmail.com, [b]robert.botet@u-psud.fr

Corresponding author: Rakesh K. Rai, rakesh2273@gmail.com

PACS 78.67.Sc, 78.67.Bf

ABSTRACT Spatial structures of electromagnetic near-fields generated by plasmonic resonances are studied through numerical simulations. Resonances can appear in silver nanoplates onto which nanoparticles of various shapes are deposited. For forthcoming biophysical applications, nanoparticles are considered here as irregular aggregates of grains made of DNA material. The Discrete Dipole Approximation technique is used to calculate the electromagnetic field profiles. In certain controlled physical situations, the plasmonic pattern appears to be the glowing anti-shadow of the deposited nanoparticle, and such a pattern locally produces strong increase in the electromagnetic fields. Even when the nanoparticle size is much smaller than the wavelength, fine (sub-wavelength) details of the anti-shadow are directly related to the shape of the nanoparticle. These observations should result in a better understanding of the Surface-Enhanced Raman Scattering process and an improvement in nanocharacterization techniques.

KEYWORDS light scattering, discrete dipole approximation, DNA materials, nanoparticles

FOR CITATION Rai R.K., Botet R.S. Near-field optical patterns of dielectric nanoparticles deposited on a metallic surface. *Nanosystems: Phys. Chem. Math.*, 2022, **13** (1), 56–61.

## 1. Introduction

Recent interest in the study of local electromagnetic fields near nanoobjects resulted from new developments in nanofabrication [1–3] and nanocharacterization techniques [1, 4] along with near-field scanning microscope improvements [5]. It is now clear that nanostructure shapes affect the various optical properties, hence the need to precisely study the scattering properties of non-spherical nanoparticles (NPs) in relation to their possible irregular shapes.

Electromagnetic fields near to and far from the scattering object may exhibit very different spatial distributions as well as magnitudes, even if both fields are linked together. In particular, due to coherence effect and/or plasmon oscillations, the field inside and near the nanoparticles (NPs) is often locally enhanced in comparison to the incident field. For example, Raman intensity scattered from pyridine adsorbed onto the roughened surface of noble metal (Ag, Cu or Au), is greatly enhanced [6, 7]. This Surface Enhanced Raman Spectroscopy (SERS) is essentially explained by plasmon resonance coupled to a correlated nanoscale roughness of the metallic surface. Roughness can result either of electrochemical treatment from a smooth metallic surface [6, 7] or from metallic NPs deposition on a smooth metallic surface [8, 9].

Particle detection requires EM scattering spots as intense as possible, whereas particle characterization calls for shape recognition from the observed EM scattering pattern. In this context, a novel research topic is the formation of intense sub-diffraction limited-field localization region – the photonic nanojet – in the shadow region (forward direction) of particular dielectric nanoparticles [10]. Such a nanojet depends strongly on the shape of the particle. However, this approach is, for the moment, restricted to particles made of homogeneous material with very simple shapes [11].

An efficient and versatile tool to calculate electromagnetic near-fields is the Discrete Dipole Approximation (DDA), in which the target under investigation is represented by an arrangement of identical small polarizable points (dipoles) on nodes of a simple cubic lattice, and covering the target geometry [12, 13]. The most popular corresponding numerical code is generically named: DDSCAT, and is available on Draine's website [14]. In the version DDSCAT 7.3, the electric field intensity near the scattering particles and inside it, is calculated for any arbitrary particle shape made of any dielectric material. This free software provides a valuable tool to study the distribution of the scattered electric field in the space near the particle. Hereafter, using the DDSCAT 7.3 code, we compute the electric field distribution near and inside Nps of different shapes but of same volume and made of the same dielectric material. That way, all the Nps have the same equivalent radius (that is the radius of the sphere of same volume), and only their shapes are changed. We focus our discussion on the 'electric enhancement factor', $Q = |E_{loc}/E_{inc}|^2$, here defined as the ratio between the intensity of the local scattered electric field, $E_{loc}$, and the intensity of the incident field, $E_{inc}$. For the small (*i.e.* size parameter $\ll 1$) NPs, the enhancement factor is proportional to the squared polarizability, $\alpha^2$, with $\alpha \propto (\epsilon_p - 1)/(\epsilon_p + 2)$ and $\epsilon_p$ is the dielectric constant of the particle. The largest values of $Q$ are obtained close to the Fröhlich resonance frequencies for

which the dielectric constant $\epsilon_p \simeq -2$ [15]. In this case, the global enhancement factor is proportional to the volume of the small particle, then it does not depend on the definite shape of the NP. We will see below that, when the size parameter is of order 1 or larger, the largest values of $Q$ depend on the NP shape.

In a previous study, it was observed that monodispered polystyrene NPs deposited on gold nanoplates could be detected by surface plasmon resonance [16]. Also, single stranded DNA associated with Ag nanoparticles were detected using silver film as base [17]. The present study consists of theoretical investigation of enhancement in near electric field of single nanoparticle of dielectric material aggregates in different shapes. We consider here two kinds of NPs, either isolated or deposited on a silver base, and we compare the electromagnetic near-field patterns in both cases. When the particle is deposited on a metallic surface, the enhanced electric field is clearly related to its outline, thus allowing nanocharacterization of the deposited NPs.

## 2. Method and calculation

Significant increase in the electric near-field is known for fractal metallic NPs over regular surface [18]. Although such very irregular particle shapes are of interest, we consider here two alternative kinds of shapes to keep the discussion simple:

(1) irregular compact-shape particle generated using the Reaction-Limited Particle-Cluster Aggregation model (RPCA) [19]. In this model, the NP is made by successive aggregation of monomers placed randomly on the surface of the aggregate. In a statistical average, the NP is homogeneous and its shape is spherical. (see Fig. 1, left);

(2) particle generated using a combination of Reaction-Limited Cluster-Cluster Aggregation model (RCCA) [20] for the core and Reaction-Limited Particle-Cluster Aggregation model (RPCA) [19] for the mantle, in a volume core/mantle ratio equal to 1:4. In the RCCA model, the particle is made by successive aggregation of clusters randomly sticking together, leading to a fractal core (fractal dimension = 2) of the actual NP. In a second step, the fractal arms of the RCCA cluster are made more dense by RPCA aggregation. This kind of particle is used to model insterstellar particles in an astrophysical context [21]. Details of the building process and examples are given in [22].

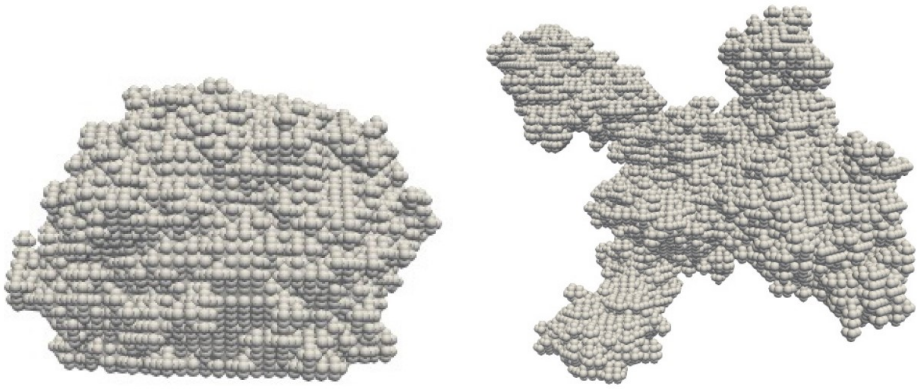

FIG. 1. Irregular compact RPCA and core-mantle particles, used in the calculations (see description in Section 2). On these figures, each small sphere represents an individual electromagnetic dipole used in the DDA method for the calculation of electromagnetic scattering.

Theoretical calculations for light scattering enhancement have been done using: 1) Discrete Dipole Approximation (DDA) method with the Clausius-Mossotti relation corrected by lattice dispersion relation and $3^{\rm rd}$ order radiative term [23] or: 2) Finite-Difference Time-Domain (FDTD) method apart from Mie theory estimates [8]. The FDTD method is used to calculate local enhancement for different non-spherical shapes for combination of dielectric and noble metals [24].

Dipole discretization required by DDSCAT code is realized using the same number of dipoles for all the particles. The values of the refractive index depend on the material (here, DNA molecule or bulk silver) and they are taken from standard available data. The wavelength of the incident light is fixed here to the value $0.354$ $\mu$m because it is close to a Frölich frequency for silver.

## 3. Results and discussion

### 3.1. Isolated DNA material aggregates

The refractive index of aggregates of DNA materials is $1.64+i1.47\times10^{-5}$ at the incident electromagnetic wavelength 0.354 $\mu$m. The electromagnetic wave propagates along the $x$-direction (see Figs. 2 and 3). Such water soluble DNA

material was allowed to be deposited on the nickel surface to form DNA film and then refractive index of the film of this DNA material was determined [25]. We use here this refractive index in the calculations.

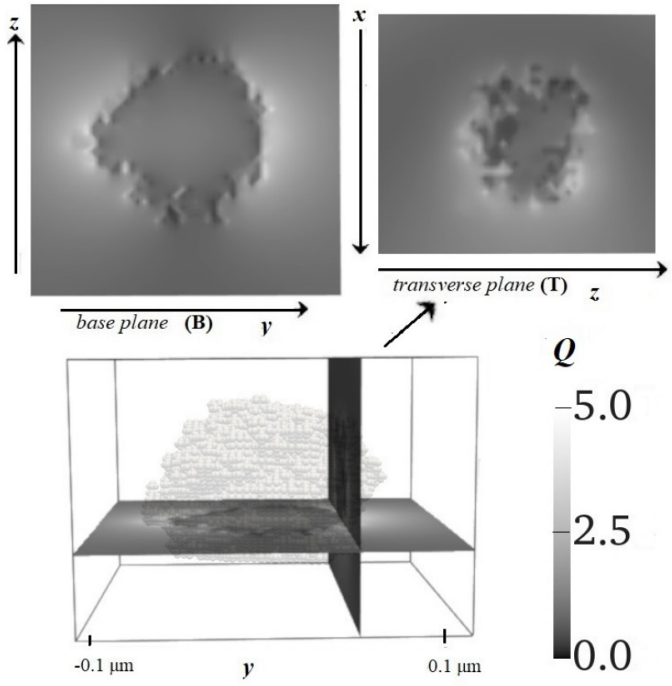


FIG. 2. Distribution of the local electric enhancement factor ( $Q = |E_{loc}/E_{inc}|^2$) near and inside an irregular compact aggregate of DNA material. The electromagnetic wave is linearly polarized along the $z$-direction. The spatial scale in both figures is in $\mu$m. The enhanced factor, $Q$, is of order 5.

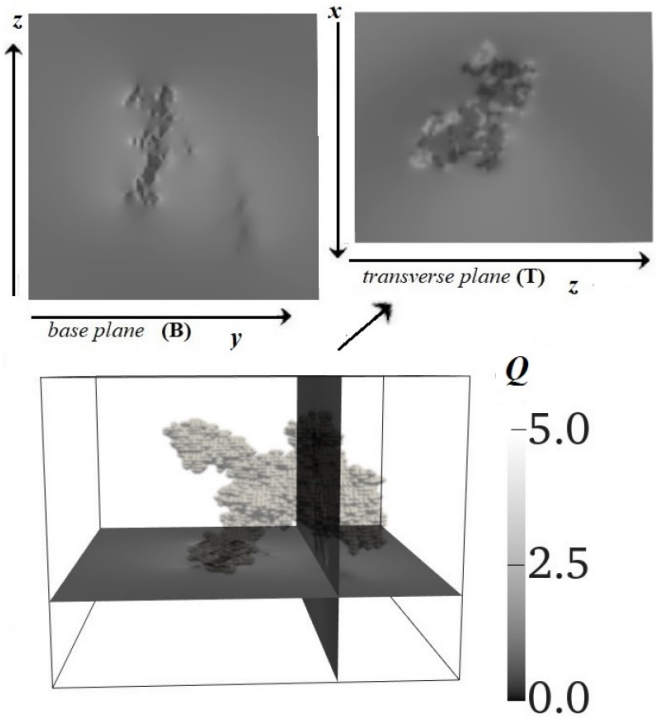


FIG. 3. Distribution of the local electric enhancement factor ($Q = |E_{loc}/E_{inc}|^2$) near and inside of a coated fractal NP of effective radius $0.06\mu$m made of DNA material. The incident electromagnetic wavelength is 0.354 $\mu$m and the EM wave propagates along the $x$-direction. It is polarized along the $z$-direction. The spatial scale in both figures is in $\mu$m. The enhanced factor, $Q$, is of order 5.

- The isolated irregular compact (RPPA) particle

  On the top of Fig. 2, the electric enhancement factor, $Q = |E_{loc}/E_{inc}|^2$, is plotted inside and around the DNA aggregates' spheres of effective radius $a = 0.06$ $\mu$m for the electromagnetic wavelength $\lambda = 0.354$ $\mu$m. The value of the size parameter $x = 2\pi a/\lambda$ is then close to 1. The calculations are performed for an electromagnetic wave incident along the $x$-axis. The total number of dipoles representing the RPPA particle of DNA aggregates is 10012. To show more clearly the enhancement, two planes are considered in which base plane is perpendicular to the incident EM radiation.
- The isolated random coated fractal particle

  The RPCA-RCCA combination (see [22] for details and examples) generating a coated fractal particle made of 9908 dipoles, yields a very different electric field magnitude distribution (see Fig. 3), as it does not show any resemblance with the previous profile seen in Fig. 2. The values of the enhancement factor, $Q$ are nearly the same. It is clear here that the intensity distribution depends on the shape of the particle.

### 3.2. Nanoparticles of DNA material deposited on a silver substrate

We now consider the same two particles as in Fig. 1 deposited on a silver base. The DDSCAT calculations are considerably heavier than the case of a free particle because we have to manage the electromagnetic response of the whole silver substrate. Therefore, for this part of the study, we placed the same DNA material NPs as before on the silver nano-plate of dimensions $300 \times 300 \times 50$ nm. This silver nanoplate is represented by $66 \times 66 \times 11$ $(47916)$ dipoles. The graphical results are shown on Figs. 4 and 5.

Some important conclusions can be drawn from these profiles:

- Particles deposited on silver substrate exhibit a much larger electric enhancement of the near-field electric intensity compared to the case of the isolated particles. The mean value of this enhancement reaches a factor $\simeq 90$ for the particles in this case.
- The electric field pattern of the dielectric particle deposited on the silver substrate exhibits a glowing anti-shadow in the near-field region along the forward direction (Fig. 4), instead of the ordinary dark shadow as it is the case when there is no silver base. This anti-shadow is the result of plasmon resonance in the metallic base in the vicinity of the NP.

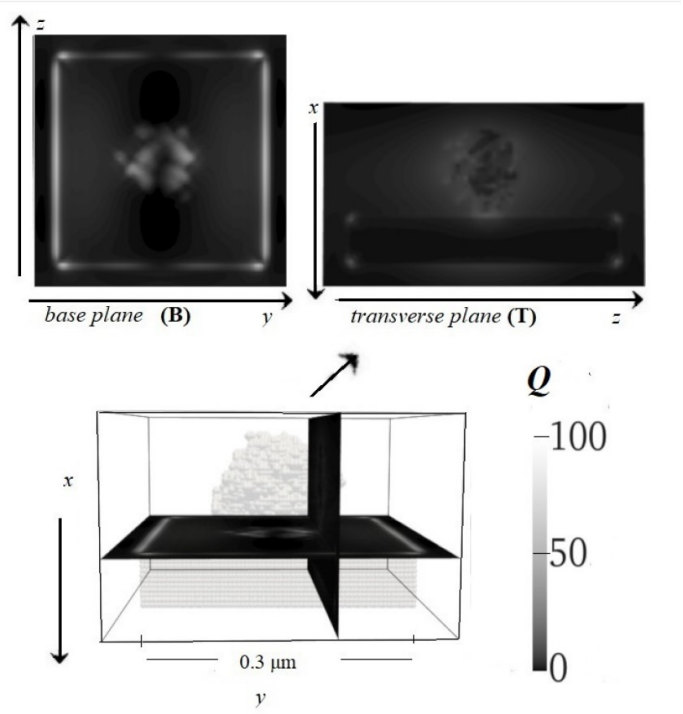


FIG. 4. Distribution of the local electric enhancement factor, ($Q = |E_{loc}/E_{inc}|^2$), for an irregular compact NP made of DNA material on a silver base. The glowing 'anti-shadow' appears as the enhanced brightness in the shadow position (that is near-field in the forward scattering direction) . Unlike the case of the isolated particles, the electric field intensity of the anti-shadow is significantly larger (more than 90 times larger).

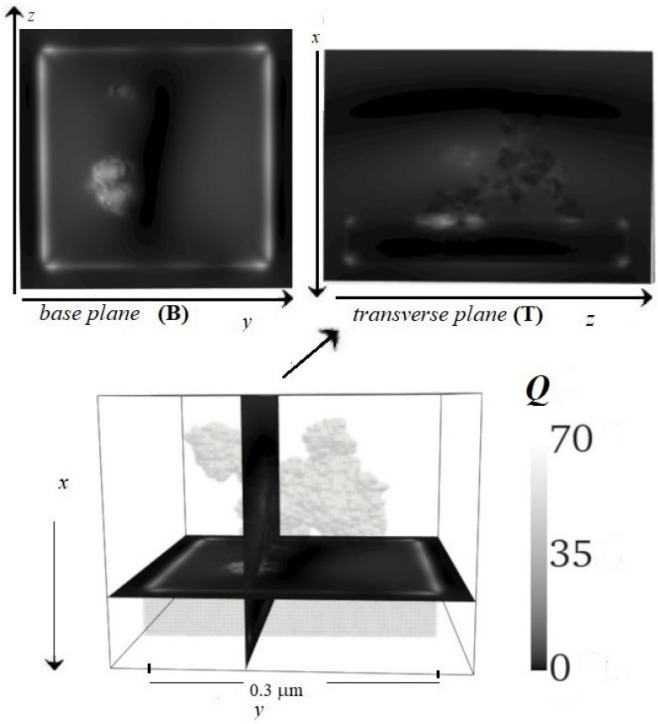


FIG. 5. Distribution of the local electric enhancement factor, ($Q = |E_{loc}/E_{inc}|^2$), for an irregular coated-fractal NP of DNA material on the silver base. Similarly to the irregular compact NP (Fig. 4), the electric field intensity of the anti-shadow part is here more than 70 times larger than the intensity of the incident field.

- Anti-shadow pattern is present for both the irregular compact and the coated fractal NP, but their geometrical structures are different. Thus, one can conclude that the shape of the anti-shadow pattern depends on the geometrical shape of the NPs.

These conclusions may be important for applications, either for nanocharacterization of NPs or for NPs detection. Indeed, using a simple protocol, definite information about the morphology of a single NP can be deduced from experimental analysis of its anti-shadow pattern, when the particle is deposited on a silver base at a wavelength close to Frölich frequency. Let us be more precise. We do not know any way to inverse mathematically the near-field pattern of the electromagnetic field scattered by a single particle to rebuild its exact geometrical shape. This fundamental flaw is shared with other domains of NP characterization, e.g. Small-Angle X-ray Scattering (SAXS) analysis [26]. However, the same technical method as in SAXS can be used, that is:

(1) generate various possible models of particles (e.g. through computer simulations);
(2) calculate the near-field anti-shadow for particles of each model deposited on a silver base (we showed that DDSCAT numerical code can be used efficiently to complete this task);
(3) experimentally measure the anti-shadow patterns generated by real NPs adsorbed onto the silver substrate and compare them to the models. The experimental part of the latter task could be done using Scanning Near-field Optical Microscope (SNOM) (e.g. [27]).

We have seen that two particles of different shapes exhibited very different anti-shadow patterns, then the protocol proposed above is expected to be sensitive to the particle shape.

## 4. Conclusion

In this article, we presented numerical calculations of light scattering by nanometer-sized dielectric particles deposited on a metal substrate, and we showed that the definite shape of the particle has a strong effect in the resulting near-field profile at a sub-wavelength scale. Actually, different shapes were seen to leave their own imprints on a silver base as particular anti-shadows, that is of strongly enhanced (glowing) local fields generated by surface plasmons. Therefore, the silver nanoplate serves as a base to detect enhancement in the local EM field around the dielectric material. Characterization of NP shapes can, in principle, be extracted from such anti-shadow images, even if only by comparing Scanning Near-field Optical Microscope images with anti-shadows calculated from relevant particle models. If the size of the NP is too small to use such scanning technique, the very large enhancement of the field intensity allows one to consider direct detection of the glowing anti-shadow as the signature of the NP deposited on the silver base.

## References


[1] Pana X., Medina-Ramirez I., Mernaugh R., Liu J. Nanocharacterization and bactericidal performance of silver modified titania photocatalyst. *Colloids and Surfaces B: Biointerfaces*, 2010, **77**, P. 82–89.

[2] Gates B.D., Xu Q., et al. New approaches to nanofabrication: molding, printing, and other techniques. *Chem. Rev.*, 2005, **105**, P. 1171–1196.

[3] Biswas A., Bayer I.S., et al. Advances in top-down and bottom-up surface nanofabrication: techniques, applications & future prospects. *Advances in Colloid and Interface Science*, 2012, **170**, P. 2–27.

[4] Gillet J.-N., Meunier M. General Equation for Size Nanocharacterization of the Core-Shell Nanoparticles by X-ray Photoelectron Spectroscopy. *J. Phys. Chem. B*, 2005, **109**, P. 8733–8737.

[5] Betzig E., Trautman J.K. Near-Field Optics: Microscopy, Spectroscopy, and Surface Modification Beyond the Diffraction Limit. *Science*, 1992, **257**, P. 189–195.

[6] Jeanmaire D.L., Van Duyne R.P. Surface raman spectroelectrochemistry: Part I. Heterocyclic, aromatic, and aliphatic amines adsorbed on the anodized silver electrode. *J. of Electroanalytical Chemistry and Interfacial Electrochemistry*, 1977, **84**, P. 1–20.

[7] Albrecht M.G., Creighton J.A. Anomalously intense Raman spectra of pyridine at a silver electrode. *J. Am. Chem. Soc.*, 1977, **99**, P. 5215–5217.

[8] Schatz G.C., Young M.A., Van Duyne R.P. Electromagnetic mechanism of SERS. In: Kneipp K., Moskovits M. & Kneipp H.(Eds.) Surface-Enhanced Raman Scattering – Physics and Applications. Topics Apl. Phys., 2006, **103**, P. 19–46.

[9] Stiles P.L., Dieringer J.A., Shah N.C., Van Duyne R.P. Surface-enhanced Raman spectroscopy. *Annu. Rev. Anal. Chem.*, 2008, **1**, P. 601–626.

[10] Zhu J., Goddard L.L. All-dielectric concentration of electromagnetic fields at the nanoscale: the role of photonic nanojets. *Nanoscale Adv.*, 2019, **1**, P. 4615–4643.

[11] Jia Y., Li R., Zhuanga W., Liang J. Photonic nanojet generated by a spheroidal particle illuminated by a vector Bessel beam. *Results in Optics*, 2021, **4**, 100106.

[12] Purcell E.M., Pennypacker C.R. Scattering and absorption of light by nonspherical dielectric grains. *Astrophys. J.*, 1973, **186**, P. 705–714.

[13] Draine B.T. The discrete-dipole approximation and its application to interstellar graphite grains. *Astrophys. J.*, 1988, **333**, P. 848–872.

[14] Draine B.T. The Discrete Dipole Approximation for Scattering and Absorption of Light by Irregular Particles. URL: https://www.astro.princeton.edu/˜draine/DDSCAT.7.3.html.

[15] Anderson M.S. Enhanced infrared absorption with dielectric nanoparticles. *Appl. Phys. Lett.*, 2003, **83**, P. 2964–2966.

[16] Zybin A., Kuritsyn Y.A., et al. Real-time Detection of Single Immobilized Nanoparticles by Surface Plasmon Resonance Imaging. *Plasmonics*, 2009, **5** (1), P. 31–35.

[17] Braun G., Lee S.J., et al. Surface-Enhanced Raman Spectroscopy for DNA Detection by Nanoparticle Assembly onto Smooth Metal Films. *J. Am. Chem. Soc.*, 2007, **129**, P. 6378–6379.

[18] Shalaev V.M., Botet R., Mercer J., Stechel E.B. Optical properties of self-affine thin films. *Phys. Rev. B*, 1996, **54**, P. 8235–8242.

[19] Jullien R., Botet R. *Aggregation and Fractal Aggregates*. World Scientific Publishing, Singapore, 1987, 130 p.

[20] Meakin P., Jullien R. The effects of restructuring on the geometry of clusters formed by diffusion-limited, ballistic, and reaction-limited cluster-cluster aggregation. *J. Chem. Phys.*, 1988, **89**, P. 246–250.

[21] Rai R.K., Rastogi S., Botet R. Effect of grain shape on extinction using effective medium theory. *Asian J. of Physics*, 2015, **24**, P. 1097–1103.

[22] Rai R.K., Botet R.S. *Monthly Notices of the Royal Astron. Society*, 2014, **444**, P. 303–312.

[23] Draine B.T., Goodman J. Beyond Clausius-Mossotti – Wave propagation on a polarizable point lattice and the discrete dipole approximation. *Astrophys. J.*, 1993, **405**, P. 685–697.

[24] Abdulhalim I. Coupling configurations between extended surface electromagnetic waves and localized surface plasmons for ultrahigh field enhancement. *Nanophotonics*, 2018, **7** (12), P. 1891–1916.

[25] Inagaki T., Hamm R.N., Arakawa E.T. Optical and dielectric properties of DNA in the extreme ultraviolet, *The J. of Chemical Physics*, 1974, **61**, P. 4246–4250.

[26] Pedersen J.S. Analysis of small-angle scattering data from colloids and polymer solutions: modeling and least-squares fitting. *Advances in Colloid and Interface Science*, 1997, **70**, P. 171–210.

[27] Oshikane Y., Kataoka T., et al. Observation of nanostructure by scanning near-field optical microscope with small sphere probe. *Science and Technology of Advanced Materials*, 2007, **8**, P. 181–185.


*Submitted 11 December 2021; revised 22 December 2021; accepted 23 December 2021*

*Information about the authors:*

*Rakesh K. Rai* – RLSY College (Bettiah), B. R. A. Bihar University, Muzaffarpur, India; ORCID 0000-0003-4368-5276; rakesh2273@gmail.com

*Robert S. Botet* – Université Paris-Saclay, Laboratoire de Physique des Solides, CNRS UMR8502 , 91405 Orsay, France; ORCID 0000-0002-8515-111X; robert.botet@u-psud.fr

*Conflict of interest*: the authors declare no conflict of interest.

*Availability of data and material*: The numerical calculations were performed on PC. The data are available free of charge on request from the authors.

*Code availability*: To realize this work, we used the softwares: DDSCAT, PARAVIEW and MAYAVI which are freely available.